

EQUILIBRIUM OF ELASTIC HOLLOW INHOMOGENEOUS CYLINDERS WITH A CROSS-SECTION IN THE FORM OF CONVEX SEMI-CORRUGATIONS

The paper presents solution of a three-dimensional boundary-value stress problem of the theory of elasticity for hollow inhomogeneous orthotropic cylinders with a cross-section in the form of convex semi-corrugations with zones of large curvature. The boundary conditions at the cylinder ends make it possible to separate variables along the length. The additional functions are included into the resolving system of differential equations. These functions enable the variables to be separated along a directrix using discrete Fourier series. The boundary-value problem derived for the system of ordinary differential equations is solved by the stable numerical method of discrete orthogonalization over the cylinder thickness. The results in the form of plots and tables are presented.

1. Introduction. Problems on the stress state of circular cylinders under mechanical and thermal loads have been considered earlier by Timoshenko [16]. In the review of Soldatos [15] it is pointed out that noncircular cylindrical shells with small or large eccentricity are widely used in aerospace and mechanical engineering applications. It is also noted that the number of studies devoted to noncircular cylinders is rather scanty in comparison with the extended literature on circular cylinders. However, in contrast to circular cylinders, where in solving the boundary-value problems the dimensionality may be reduced by representing the resolving functions in the form of Fourier series along a circumferential coordinate, the problem solution in the case of noncircular cylinders is complicated, making it necessary to solve a three-dimensional problem.

Employment of the approaches based on various simplified physical assumptions is not always justified, making it necessary to consider this class of problems in a spatial formulation. To obtain a rather accurate solution of the problem on the equilibrium of noncircular cylinders, it is necessary to have a particular kind of apparatus combining analytical transformations, which make it possible to reduce the dimensionality of the problem, and the stable numerical method of integrating ordinary differential equations.

Of especial interest is study of the stress state in hollow cylinders with complex-shaped cross-section. In particular, this class of shells includes cylinders with cross-section in the form of joined together convex semi-corrugations such ones as that being addressed in the present paper. In certain works (e.g., [8]), the semi-corrugations are described by a segment of a sphere or a segment of a sinusoid, where at the points of conjugation, the discontinuities of derivatives of these curves hold. This rules out the possibility the condition of semi-corrugation conjunction to be satisfied. In this connection it is necessary to assign such function that makes it possible to describe the cylinder cross-section with allowance for continuity of derivatives. In the present paper we adopt, as such curve, a shortened epicycloid [6] assuming that the cylinders at the points of conjugation are highly curved.

The present paper presents solution of a new intrinsic problem of the spatial theory of elasticity for hollow layered inhomogeneous cylinders whose cross-section has the shape of convex semi-corrugations with zones of large curvature. The solution of this problem is of great theoretical interest and has applied importance. In solving the problem, the nontraditional approach with employment of discrete Fourier series (see [5, 12] and [13]) and stable numerical method of discrete orthogonalization ([1, 2, 10] and [4]) are used.

2. Problem statement. Let us consider a spatial stress problem for elastic hollow layered noncircular constant-thickness cylinders with the cross-section at each point having the form of a shortened epicycloid [7, 14].

We choose the orthogonal curvilinear coordinate system s, ψ, γ , where s is the arc length along a generatrix, ψ is the polar angle at the cross-section, γ is the normal coordinate along the thickness of the cylinder.

The curve equation at the cross-section of the reference surface is specified in the parametrical form as follows:

$$\begin{aligned} x &= (A + a) \cos \psi - \lambda a \cos\left(\frac{A + a}{a} \psi\right), \\ y &= (A + a) \sin \psi - \lambda a \sin\left(\frac{A + a}{a} \psi\right), \end{aligned} \quad (1)$$

where A is the radius of the fixed circumference, a ($a > 0$) is the radius of the moving circumference, $\lambda < 1$ is the distance to the radius of the moving circumference, ψ is the angular parameter ($0 < \psi < 2\pi$) that makes up the central angle at the cross-section (Fig. 1). In this case the first quadratic form can be written as

$$dS^2 = ds^2 + A_2^2(\psi, \gamma) d\psi^2 + d\gamma^2, \quad (2)$$

where

$$\begin{aligned} A_2(\psi, \gamma) &= A_2 = H_2(\psi, \gamma) \omega(\psi), & H_2(\psi, \gamma) &= H_2 = 1 + \gamma/R(\psi), \\ \omega(\psi) &= \omega = \sqrt{\left(\frac{dx}{d\psi}\right)^2 + \left(\frac{dy}{d\psi}\right)^2}. \end{aligned} \quad (3)$$

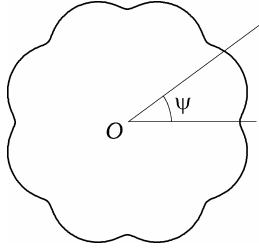


Fig. 1

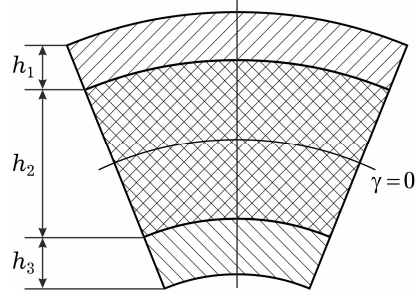


Fig. 2

Here $R(\psi)$ is the curvature radius of the curve at the cross-section:

$$R_\psi = R(\psi) = \frac{(A + a) \left(1 + \lambda^2 - 2\lambda \cos\left(\frac{A + a}{a} \psi\right)\right)^{3/2}}{1 + \lambda^2 \left(\frac{A + a}{a}\right) - \lambda \left(\frac{A + 2a}{a}\right) \cos\left(\frac{A + a}{a} \psi\right)}. \quad (4)$$

Let the cylinders be hollow and composed of three rigidly joined (Fig. 2) (without slip and separation) layers under the uniform load $q_\gamma = q_0 \sin(\pi s/\ell)$ ($q_0 = \text{const}$) applied to the external surface. The material of each layer is inhomogeneous over the thickness and homogeneous along the generatrix and directrix. According to the conditions of joint operation of the layers the stresses $\sigma_\gamma, \tau_{s\gamma}, \tau_{\psi\gamma}$ and displacements u_γ, u_s, u_ψ on the interface between the i -th and $(i + 1)$ -th layers should be continuous. Then, at $\gamma = \gamma_i$ we have:

$$\begin{aligned} \sigma_\gamma^i &= \sigma_\gamma^{i+1}, & \tau_{s\gamma}^i &= \tau_{s\gamma}^{i+1}, & \tau_{\psi\gamma}^i &= \tau_{\psi\gamma}^{i+1}, \\ u_\gamma^i &= u_\gamma^{i+1}, & u_s^i &= u_s^{i+1}, & u_\psi^i &= u_\psi^{i+1}. \end{aligned} \quad (5)$$

Taking into account (1)–(4), we can write the basic equations of the spatial theory of elasticity, which describe the class of the problems being considered for the i -th layer, $i = 0, 1, \dots, P$, as follows:

– expressions for strains

$$\begin{aligned}
e_s^i &= \frac{\partial u_s^i}{\partial s}, & e_\psi^i &= \frac{1}{A_2^i} \frac{\partial u_\psi^i}{\partial \psi} + \frac{1}{H_2^i} \frac{\partial H_2^i}{\partial \gamma} u_\gamma^i, \\
e_\gamma^i &= \frac{\partial u_\gamma^i}{\partial \gamma}, & e_{s\psi}^i &= \frac{1}{A_2^i} \frac{\partial u_s^i}{\partial \psi} + \frac{\partial u_\psi^i}{\partial s}, \\
e_{s\gamma}^i &= \frac{\partial u_\gamma^i}{\partial s} + \frac{\partial u_s^i}{\partial \gamma}, & e_{\psi\gamma}^i &= H_2^i \frac{\partial}{\partial \gamma} \left(\frac{u_\psi^i}{H_2^i} \right) + \frac{1}{A_2^i} \frac{\partial u_\gamma^i}{\partial \psi};
\end{aligned} \tag{6}$$

– equilibrium equations

$$\begin{aligned}
H_2^i \frac{\partial \sigma_s^i}{\partial s} + \frac{1}{\omega} \frac{\partial \tau_{s\psi}^i}{\partial \psi} + \frac{\partial}{\partial \gamma} (H_2^i \tau_{s\gamma}^i) &= 0, \\
\frac{1}{\omega} \frac{\partial \sigma_\psi^i}{\partial \psi} + \frac{\partial}{\partial \gamma} (H_2^i \tau_{\psi\gamma}^i) + H_2^i \frac{\partial \tau_{s\psi}^i}{\partial s} + \frac{\partial H_2^i}{\partial \gamma} \tau_{\psi\gamma}^i &= 0, \\
\frac{\partial}{\partial \gamma} (H_2^i \sigma_\gamma^i) + H_2^i \frac{\partial \tau_{s\gamma}^i}{\partial s} + \frac{1}{\omega} \frac{\partial \tau_{\psi\gamma}^i}{\partial \psi} - \frac{\partial H_2^i}{\partial \gamma} \sigma_\psi^i &= 0;
\end{aligned} \tag{7}$$

– relations of generalized Hooke's law for an orthotropic body

$$\begin{aligned}
e_s^i &= a_{11}^i \sigma_s^i + a_{12}^i \sigma_\psi^i + a_{13}^i \sigma_\gamma^i, & e_t^i &= a_{12}^i \sigma_s^i + a_{22}^i \sigma_\psi^i + a_{23}^i \sigma_\gamma^i, \\
e_\gamma^i &= a_{13}^i \sigma_s^i + a_{23}^i \sigma_\psi^i + a_{33}^i \sigma_\gamma^i, \\
e_{\psi\gamma}^i &= a_{44}^i \tau_{\psi\gamma}^i, & e_{s\gamma}^i &= a_{55}^i \tau_{s\gamma}^i, & e_{s\psi}^i &= a_{66}^i \tau_{s\psi}^i,
\end{aligned} \tag{8}$$

where for an orthotropic material

$$\begin{aligned}
a_{11}^i &= \frac{1}{E_s^i}, & a_{12}^i &= -\frac{\nu_{s\psi}^i}{E_\psi^i} = -\frac{\nu_{\psi s}^i}{E_s^i}, & a_{13}^i &= -\frac{\nu_{s\gamma}^i}{E_\gamma^i} = -\frac{\nu_{\gamma s}^i}{E_s^i}, \\
a_{22}^i &= \frac{1}{E_\psi^i}, & a_{23}^i &= -\frac{\nu_{\gamma\psi}^i}{E_\gamma^i} = -\frac{\nu_{\psi\gamma}^i}{E_\psi^i}, \\
a_{33}^i &= \frac{1}{E_\gamma^i}, & a_{44}^i &= \frac{1}{G_{\psi\gamma}^i}, & a_{55}^i &= \frac{1}{G_{s\gamma}^i}, & a_{66}^i &= \frac{1}{G_{s\psi}^i},
\end{aligned} \tag{9}$$

for an isotropic material

$$\begin{aligned}
a_{11}^i &= a_{22}^i = a_{33}^i = \frac{1}{E^i}, \\
a_{12}^i &= a_{13}^i = a_{23}^i = -\frac{\nu^i}{E^i}, \\
a_{44}^i &= a_{55}^i = a_{66}^i = \frac{2(1 + \nu^i)}{E^i},
\end{aligned}$$

E_s^i , E_ψ^i , E_γ^i , $G_{\psi\gamma}^i$, $G_{s\gamma}^i$, $G_{s\psi}^i$, $\nu_{\psi\gamma}^i$, $\nu_{s\gamma}^i$, $\nu_{s\psi}^i$ are the corresponding elastic moduli along the coordinate axes, shear moduli, and Poisson's ratios.

Relations (6)–(8) make up the closed system of partial differential equations, which describe the stress state of the cylinders being considered in the domain ($0 \leq s \leq \ell$, $0 \leq \psi \leq 2\pi$, $\gamma_0 \leq \gamma \leq \gamma_p$). The boundary conditions on the outside and inside surfaces of the cylinders are specified as follows:

$$\begin{aligned}
\sigma_\gamma^0 &= 0, & \tau_{s\gamma}^0 &= 0, & \tau_{\psi\gamma}^0 &= 0 & \text{at} & \gamma = \gamma_0, \\
\sigma_\gamma^p &= q_\gamma, & \tau_{s\gamma}^p &= 0, & \tau_{\psi\gamma}^p &= 0 & \text{at} & \gamma = \gamma_p.
\end{aligned} \tag{10}$$

Let us consider conditions for cylinders with simply supported ends:

$$\sigma_s^i = u_\psi^i = u_\gamma^i = 0 \quad \text{at} \quad s = 0, \quad s = \ell. \quad (11)$$

As resolving functions, with allowance for the conjugation and boundary conditions, we choose the stress and displacement components σ_γ^i , $\tau_{s\gamma}^i$, $\tau_{\psi\gamma}^i$, u_γ^i , u_s^i , u_ψ^i . Upon performing some transformations, from (6)–(8) we obtain the resolving system of sixth-order partial differential equations with variable coefficients for each layer in the form

$$\begin{aligned} \frac{\partial \sigma_\gamma^i}{\partial \gamma} &= (c_2^i - 1) \frac{1}{H_2^i} \frac{\partial H_2^i}{\partial \gamma} \sigma_\gamma^i - \frac{\partial \tau_{s\gamma}^i}{\partial s} - \frac{1}{A_2^i} \frac{\partial \tau_{\psi\gamma}^i}{\partial \psi} + b_{22}^i \left(\frac{1}{H_2^i} \frac{\partial H_2^i}{\partial \gamma} \right)^2 u_\gamma^i + \\ &\quad + b_{12}^i \frac{1}{H_2^i} \frac{\partial H_2^i}{\partial \gamma} \frac{\partial u_s^i}{\partial s} + b_{22}^i \frac{1}{H_2^i A_2^i} \frac{\partial H_2^i}{\partial \gamma} \frac{\partial u_\psi^i}{\partial \psi}, \\ \frac{\partial \tau_{s\gamma}^i}{\partial \gamma} &= -c_1^i \frac{\partial \sigma_\gamma^i}{\partial s} - \frac{1}{H_2^i} \frac{\partial H_2^i}{\partial \gamma} \tau_{s\gamma}^i - b_{12}^i \frac{1}{H_2^i} \frac{\partial H_2^i}{\partial \gamma} \frac{\partial u_\gamma^i}{\partial s} - b_{11}^i \frac{\partial^2 u_s^i}{\partial s^2} - \\ &\quad - b_{66}^i \frac{1}{A_2^i} \frac{\partial}{\partial \psi} \left(\frac{1}{A_2^i} \frac{\partial u_s^i}{\partial \psi} \right) - (b_{12}^i + b_{66}^i) \frac{1}{A_2^i} \frac{\partial^2 u_\psi^i}{\partial s \partial \psi}, \\ \frac{\partial \tau_{\psi\gamma}^i}{\partial \gamma} &= -c_2^i \frac{1}{A_2^i} \frac{\partial \sigma_\gamma^i}{\partial \psi} - \frac{2}{H_2^i} \frac{\partial H_2^i}{\partial \gamma} \tau_{\psi\gamma}^i - b_{22}^i \frac{1}{A_2^i} \frac{\partial}{\partial \psi} \left(\frac{1}{H_2^i} \frac{\partial H_2^i}{\partial \gamma} u_\gamma^i \right) - \\ &\quad - (b_{12}^i + b_{66}^i) \frac{1}{A_2^i} \frac{\partial^2 u_s^i}{\partial s \partial \psi} - b_{22}^i \frac{1}{A_2^i} \frac{\partial}{\partial \psi} \left(\frac{1}{A_2^i} \frac{\partial u_\psi^i}{\partial \psi} \right) - b_{66}^i \frac{\partial^2 u_\psi^i}{\partial s^2}, \\ \frac{\partial u_\gamma^i}{\partial \gamma} &= c_4^i \sigma_\gamma^i - c_2^i \frac{1}{H_2^i} \frac{\partial H_2^i}{\partial \gamma} u_\gamma^i - c_1^i \frac{\partial u_s^i}{\partial s} - c_2^i \frac{1}{A_2^i} \frac{\partial u_\psi^i}{\partial \psi}, \\ \frac{\partial u_s^i}{\partial \gamma} &= a_{55}^i \tau_{s\gamma}^i - \frac{\partial u_\gamma^i}{\partial s}, \quad \frac{\partial u_\psi^i}{\partial \gamma} = a_{44}^i \tau_{\psi\gamma}^i - \frac{1}{A_2^i} \frac{\partial u_\gamma^i}{\partial \psi} + \frac{1}{H_2^i} \frac{\partial H_2^i}{\partial \gamma} u_\psi^i, \end{aligned} \quad (12)$$

with the boundary conditions (10) and (11), where

$$\begin{aligned} b_{11}^i &= \frac{a_{22}^i a_{66}^i}{\Omega^i}, \quad b_{12}^i = -\frac{a_{12}^i a_{66}^i}{\Omega^i}, \\ b_{22}^i &= \frac{a_{11}^i a_{66}^i}{\Omega^i}, \quad b_{66}^i = \frac{a_{11}^i a_{22}^i - a_{12}^{i2}}{\Omega^i}, \\ \Omega^i &= (a_{11}^i a_{22}^i - a_{12}^{i2}) a_{66}^i, \quad c_1^i = -(b_{11}^i a_{13}^i + b_{12}^i a_{23}^i), \\ c_2^i &= -(b_{12}^i a_{13}^i + b_{22}^i a_{23}^i), \quad c_4^i = a_{33}^i + c_1^i a_{13}^i + c_2^i a_{23}^i. \end{aligned}$$

3. Method for solving the problem. Conditions (11) make it possible to reduce the dimensionality of the problem by separating the variables along the generatrix and representing the components of the resolving functions and loads as expansions into the Fourier series along the coordinate s (in what follows, for simplicity, the index i will be omitted):

$$\begin{aligned} X(s, \psi, \gamma) &= \sum_{n=1}^N X_n(\psi, \gamma) \sin \lambda_n s, \\ Y(s, \psi, \gamma) &= \sum_{n=0}^N Y_n(\psi, \gamma) \cos \lambda_n s, \end{aligned} \quad (13)$$

where

$$X = \{\sigma_\gamma, \tau_{\psi\gamma}, u_\gamma, u_\psi, q_\gamma\}, \quad Y = \{\tau_{s\gamma}, u_s\}, \quad \lambda_n = \frac{\pi n}{\ell}, \quad 0 \leq s \leq \ell.$$

Substituting (13) in system (12) and boundary conditions (10), (11), upon separating the variables, we arrive at the two-dimensional boundary-value problem for the amplitude values of expansions (13).

To reduce the two-dimensional boundary-value problem to a one-dimensional one, we will use an approach based on the application of discrete Fourier series. To this end, we change products of the resolving functions and coefficients that hinder separation of variables along the directrix with new additional functions (the index n is omitted):

$$\begin{aligned} \varphi_1^j &= \frac{1}{H_2} \frac{\partial H_2}{\partial \gamma} \left\{ \sigma_\gamma; \tau_{s\gamma}; u_\gamma; u_s; \frac{1}{H_2} \frac{\partial H_2}{\partial \gamma} u_\gamma \right\}, \quad j = 1, \dots, 5, \\ \varphi_2^j &= \frac{1}{H_2} \frac{\partial H_2}{\partial \gamma} \{ \tau_{\psi\gamma}; u_\psi \}, \quad j = 1, 2, \\ \varphi_3^j &= \frac{1}{A_2} \left\{ \frac{\partial \sigma_\gamma}{\partial \psi}; \frac{\partial u_\gamma}{\partial \psi}; \frac{\partial u_s}{\partial \psi} \right\}, \quad j = 1, 2, 3, \\ \varphi_4^j &= \frac{1}{A_2} \left\{ \frac{\partial \tau_{\psi\gamma}}{\partial \psi}; \frac{\partial u_\psi}{\partial \psi}; \frac{1}{H_2} \frac{\partial H_2}{\partial \gamma} \frac{\partial u_\psi}{\partial \psi} \right\}, \quad j = 1, 2, 3, \\ \varphi_5 &= \frac{1}{A_2} \frac{\partial}{\partial \psi} \varphi_1^3, \quad \varphi_6 = \frac{1}{A_2} \frac{\partial}{\partial \psi} \varphi_3^3, \quad \varphi_7 = \frac{1}{A_2} \frac{\partial}{\partial \psi} \varphi_4^2. \end{aligned} \quad (14)$$

Thus, the resolving system of equations with the additional functions becomes:

$$\begin{aligned} \frac{\partial \sigma_\gamma}{\partial \gamma} &= (c_2 - 1)\varphi_1^1 + \lambda_n \tau_{\psi\gamma} - \varphi_4^1 + b_{22}\varphi_1^5 + b_{12}\lambda_n \varphi_1^4 + b_{22}\varphi_4^3, \\ \frac{\partial \tau_{s\gamma}}{\partial \gamma} &= -c_1 \lambda_n \sigma_\gamma + b_{11} \lambda_n^2 u_s - \varphi_1^2 - b_{12} \lambda_n \varphi_1^3 - b_{66} \varphi_6 - (b_{12} + b_{66}) \lambda_n \varphi_4^2, \\ \frac{\partial \tau_{\psi\gamma}}{\partial \gamma} &= b_{66} \lambda_n^2 u_\psi - c_2 \varphi_3^1 - 2\varphi_2^1 - b_{22} \varphi_5 - (b_{12} + b_{66}) \lambda_n \varphi_3^3 - b_{22} \varphi_7, \\ \frac{\partial u_\gamma}{\partial \gamma} &= c_4 \sigma_\gamma + c_1 \lambda_n u_s - c_2 \varphi_4^2 - c_2 \varphi_1^3, \\ \frac{\partial u_s}{\partial \gamma} &= a_{55} \tau_{s\gamma} - \lambda_n u_\gamma, \quad \frac{\partial u_\psi}{\partial \gamma} = a_{44} \tau_{\psi\gamma} - \varphi_3^2 + \varphi_2^2, \end{aligned} \quad (15)$$

with the boundary conditions

$$\begin{aligned} \sigma_\gamma = 0, \quad \tau_{s\gamma} = 0, \quad \tau_{\psi\gamma} = 0 \quad \text{at} \quad \gamma = \gamma_0, \\ \sigma_\gamma = q_\gamma, \quad \tau_{s\gamma} = 0, \quad \tau_{\psi\gamma} = 0 \quad \text{at} \quad \gamma = \gamma_P. \end{aligned} \quad (16)$$

Including additional functions (14), we arrive at the system of equations whose coefficients formally are independent of the coordinate ψ that makes it possible to separate the variables along the directrix by representing the resolving functions, additional functions, and load components in the form of expansions into Fourier series along the directrix:

$$\tilde{X}(\psi, \gamma) = \sum_{k=0}^K \tilde{X}_k(\gamma) \cos k\psi, \quad \tilde{Y}(\psi, \gamma) = \sum_{k=1}^K \tilde{Y}_k(\gamma) \sin k\psi, \quad (17)$$

where

$$\tilde{X} = \{\sigma_\gamma, \tau_{s\gamma}, u_\gamma, u_s, \varphi_1^j, \varphi_4^j, \varphi_6, q_\gamma\}, \quad \tilde{Y} = \{\tau_{\psi\gamma}, u_\psi, \varphi_2^j, \varphi_3^j, \varphi_5, \varphi_7\}.$$

After substituting expansions (17) into the resolving system of equations (15) and corresponding boundary conditions (16) and separating the variables, we arrive at the system of ordinary differential equations with respect to the amplitude values of expansions (17):

$$\begin{aligned}
\frac{d\sigma_{\gamma,k}}{d\gamma} &= (c_2 - 1)\varphi_{1,k}^1 + \lambda_n \tau_{s\gamma,k} - \varphi_{4,k}^1 + b_{22}\varphi_{1,k}^5 + b_{12}\lambda_n \varphi_{1,k}^4 + b_{22}\varphi_{4,k}^3, \\
\frac{d\tau_{s\gamma,k}}{d\gamma} &= -c_1\lambda_n \sigma_{\gamma,k} + b_{11}\lambda_n^2 u_{s,k} - \varphi_{1,k}^2 - b_{12}\lambda_n \varphi_{1,k}^3 - \\
&\quad - b_{66}\varphi_{6,k} - (b_{12} + b_{66})\lambda_n \varphi_{4,k}^2, \\
\frac{d\tau_{\psi\gamma,k}}{d\gamma} &= b_{66}\lambda_n^2 u_{\psi,k} - c_2\varphi_{3,k}^1 - 2\varphi_{2,k}^1 - b_{22}\varphi_{5,k} - (b_{12} + b_{66})\lambda_n \varphi_{3,k}^3 - b_{22}\varphi_{7,k}, \\
\frac{du_{\gamma,k}}{d\gamma} &= c_4\sigma_{\gamma,k} + c_1\lambda_n u_{s,k} - c_2\varphi_{4,k}^2 - c_2\varphi_{1,k}^3, \\
\frac{du_{s,k}}{d\gamma} &= a_{55}\tau_{s\gamma,k} - \lambda_n u_{\gamma,k}, \\
\frac{du_{\psi,k}}{d\gamma} &= a_{44}\tau_{\psi\gamma,k} - \varphi_{3,k}^2 + \varphi_{2,k}^2, \quad k = 0, \dots, K,
\end{aligned} \tag{18}$$

with the boundary conditions

$$\begin{aligned}
\gamma = \gamma_0 : \quad & \sigma_{\gamma,k} = 0, \quad \tau_{s\gamma,k} = 0, \quad \tau_{\psi\gamma,k} = 0, \\
\gamma = \gamma_P : \quad & \sigma_{\gamma,k} = q_{\gamma,k}, \quad \tau_{s\gamma,k} = 0, \quad \tau_{t\gamma,k} = 0.
\end{aligned} \tag{19}$$

Equations of system (18) are integrated simultaneously for all harmonics of expansions (17).

The amplitude values $\varphi_{m,k}^j$ of additional functions which enter into (18) are calculated by integrating system (18) at each step for $\gamma = \text{const}$ using the current values of the resolving functions. The relations that define the connectedness of all the equations of system (18) take the form

$$\begin{aligned}
\varphi_{1,k}^j &= \varphi_{1,k}^j \{ \gamma; \sigma_{\gamma,\ell}; \tau_{s\gamma,\ell}; u_{\gamma,\ell}; u_{s,\ell} \}, \quad j = 1, \dots, 5, \\
\varphi_{2,k}^j &= \varphi_{2,k}^j \{ \gamma; \tau_{\psi\gamma,\ell}; u_{\psi,\ell} \}, \quad j = 1, 2, \\
\varphi_{3,k}^j &= \varphi_{3,k}^j \{ \gamma; \sigma_{\gamma,\ell}; u_{\gamma,\ell}; u_{s,\ell} \}, \quad j = 1, 2, 3, \\
\varphi_{4,k}^j &= \varphi_{4,k}^j \{ \gamma; \tau_{\psi\gamma,\ell}; u_{\psi,\ell} \}, \quad j = 1, 2, 3, \\
\varphi_{5,k} &= \varphi_{5,k} \{ \gamma; u_{\gamma,\ell} \}, \quad \varphi_{6,k} = \varphi_{6,k} \{ \gamma; u_{s,\ell} \}, \\
\varphi_{7,k} &= \varphi_{7,k} \{ \gamma; u_{\psi,\ell} \}, \quad \ell = 0, \dots, K.
\end{aligned} \tag{20}$$

Equations of system (18) are integrated by the stable numerical method of discrete orthogonalization using the Runge-Kutta method with orthogonalization of the solutions at separate points of the interval $\gamma_0 < \gamma < \gamma_P$. Values of the additional functions are calculated by expressions (14) at each succeeding step of integration at certain points on the interval $[0, 2\pi]$. The discretely specified functions derived in such a way are used to construct the

Fourier series whose amplitude values are substituted into the resolving system of equations (18) after which the next step of integration is conducted. At the beginning of integration, using the associated values of the resolving functions with (19), the amplitude values of additional functions are determined.

The approach, which involves the discrete-orthogonalization method and the discrete Fourier series, makes it possible to solve problems rather accurately since, as the number of points, where values of additional functions are calculated, increases, the discrete Fourier series becomes progressively less distinguished from the exact Fourier series [9]. The convergence of the solutions of the equilibrium problem for cylinders of a complex-shaped cross-section obtained with the above approach, depending on the number of points of orthogonalization, points, at which tabulated values of additional functions (14) are calculated, and on the number of terms retained in expansions (17), was demonstrated in [12].

4. Numerical results and discussion. Based on the above approach, we will analyze the stress state of hollow three-layered cylinders, which have a cross-section in the form of convex semi-corrugations, under the uniform load $q_\gamma = q_0 \sin(\pi s/\ell)$, $q_0 = \text{const}$. The cylinder thickness H is $h_1 + h_2 + h_3$, where h_1 and h_3 are the thicknesses of the internal and external layers, respectively, h_2 is the thickness of the middle layer. The problem is solved for $h_1 = h_3 = 2$, $h_2 = 4$, and the cylinder length $\ell = 60$. The parameters of the cross-section of the shortened epicycloid (Fig. 1) are equal to: $A = 16$, $a = 2$ and $a = 4$, $\gamma = 0.4$. At first, we will consider the problem involving cylinders with isotropic layers, when the elastic moduli of the external and internal layers are $E_s = E_\gamma = E_0$, the elastic modulus of the middle layer is $E_\psi = dE_0$ ($d = 0.1, 0.25, 0.5, 1.0$). For all the layers we used Poisson's ratio $\nu = 0.3$. In the second case, the middle layer is orthotropic with the following parameters [7]: $E_s = 3.68E_0$, $E_\psi = 2.68E_0$, $E_\gamma = 1.1E_0$, $\nu_{s\psi} = 0.105$, $\nu_{s\gamma} = 0.405$, $\nu_{\psi\gamma} = 0.431$, $G_{s\psi} = 0.5E_0$, $G_{s\gamma} = 0.45E_0$, $G_{\psi\gamma} = 0.41E_0$.

Results of the problem solution are presented in Fig. 3–5 and Tables 1–3. Fig. 3a,b show the distributions of stresses σ_ψ along the cylinder directrix on the external and internal surfaces for $a = 2$ and $a = 4$. Here, in the case of isotropic material, solid lines with symbols correspond to the external surface, without symbols to the internal surface, dashed ones to the middle orthotropic layer. In Fig. 3a, the curves are presented in the interval $0 < \psi < \pi/8$, in Fig. 3b in the interval $0 < \psi < \pi/4$.

Fig. 3a, b shows how the inhomogeneity of the structure, mechanical properties of the material, and corrugation frequency affect the distribution of stresses along the directrix. As it is seen from Fig. 3a, the stresses σ_ψ peak at $\psi = 0$ on the external surface of the cylinder with the middle soft isotropic layer for $d = 0.1$ and are minimum when this layer is orthotropic. The stresses σ_ψ on the internal surface peak at $\psi = \pi/8$ demonstrating the same dependency as on the external surface. The similar situation holds at $a = 4$ (Fig. 3b). It should be noted that the stresses have peaked values in cylinders with the orthotropic middle layer, homogeneous and with isotropic soft middle layer in the following ratios: **1**) on the external surface at $a = 2$ as 0.59 : 1 : 1.71; **2**) on the internal surface at $a = 2$ as 0.71 : 1 : 1.54; **3**) on the external surface at $a = 4$ as 0.79 : 1 : 1.89; **4**) on the internal surface at $a = 4$ as 0.74 : 1 : 1.72.

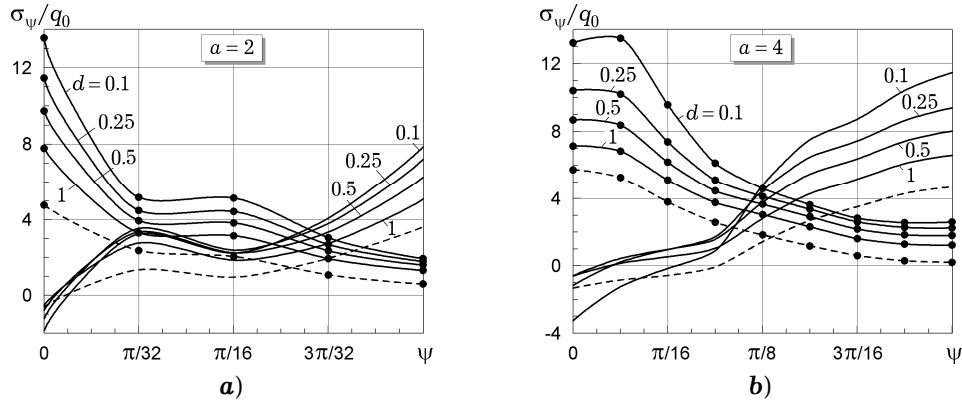


Fig. 3. Distribution of stresses σ_ψ/q_0 along the directrix on the internal and external surfaces of the cylinder for various values of a .

From the plots and relations presented it follows that values of the stresses on the external surface of the isotropic cylinders weakly depend on the corrugation sizes (in this case a number of corrugations decreases) whereas in the cylinders with the orthotropic middle layer they increase significantly. However, the difference on the internal surface reaches 20–30%. The minimum values of the stresses increase almost by a factor of 1.5, whence it follows that the load in the cylinder with eight corrugations ($a = 2$) is distributed more uniformly than in the cylinder with four corrugations ($a = 4$).

As for the distribution of stresses σ_ψ over the cylinder thickness (see Fig. 4 and 5, notation is the same), it should be noted the following. Fig. 4a,b show the distributions of stresses for $a=2$ and $a=4$ at the valley of the corrugation ($\psi = 0$), where they take maximum values. From Fig. 4a we can see that the stresses for three variants of the middle layer up to the middle thickness are equal to zero and peak (compressive stresses) on the upper boundary of the middle layer ($\gamma = 2$), the stress reaches the largest value at $d = 0.1$.

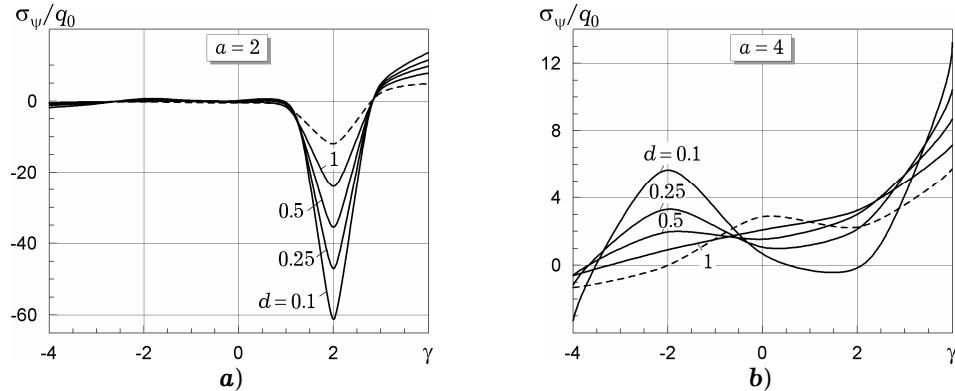


Fig. 4. Distribution of stresses σ_ψ/q_0 over the cylinder thickness at the corrugation valley for various values of a .

If $a = 4$ (Fig. 4b), the character of the stress distribution over the cylinder thickness changes. At $\gamma = -2$, the stresses on the lower boundary of the middle layer by this time are nonzero and reach the half of the peak values on the upper boundary of the middle layer at $\gamma = 2$. The stresses peak reaches in the case of a soft layer at $d = 0.1$.

The differences in the stress distributions at $a = 2$ and $a = 4$ are caused by the influence of corrugations.

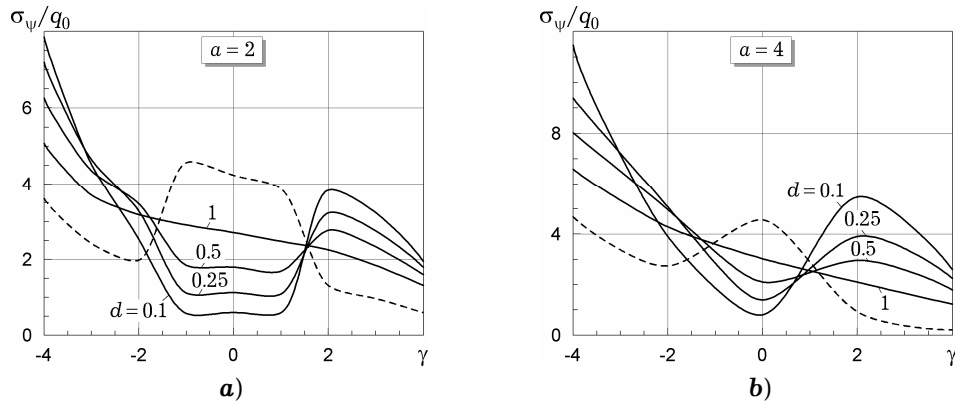


Fig. 5. Distribution of stresses σ_ψ/q_0 over the cylinder thickness at the corrugation apex for various values of a .

Fig. 5a,b demonstrate how the stresses σ_ψ are distributed at the apex of the corrugation at $a = 2$ and $a = 4$. From Fig. 5a it is seen that the stresses peak at the corrugation apex ($\psi = \pi/8$) on the internal surface at $\gamma = 4$, where the largest one corresponds to the cylinder with a soft middle layer for $d = 0.1$. As the distance to the inner surface increases, the stresses decrease and increase slightly on the upper boundary of the middle layer at $\gamma = 2$.

From Fig. 5b it follows that for $a = 4$ the stress distribution pattern over the cylinder thickness at the corrugation apex ($\psi = \pi/4$) remains close in the form to that for $a = 2$, but stresses increase roughly by a factor of 1.5. As it is seen from Fig. 4 and 5, the maximum stresses hold in the cylinder with a soft middle layer in the corrugation valley for $d = 0.1$ and $a = 2$.

Table 1

d	ψ H	$\sigma_\psi \cdot 10/q_0$					
		a = 2			a = 4		
		$\pi/32$	$2\pi/32$	$3\pi/32$	$\pi/16$	$2\pi/16$	$3\pi/16$
0.1	-4	32.31	22.26	40.64	-1.55	47.89	87.29
	-2	62.00	15.37	6.47	60.68	44.31	31.38
	0	7.06	3.55	4.26	6.63	7.72	7.36
	2	46.95	38.04	31.40	29.85	60.63	49.17
	4	51.78	51.36	30.39	95.75	46.13	28.30
0.25	-4	35.28	23.80	37.81	9.67	44.79	74.29
	-2	54.67	17.02	13.84	40.85	41.17	41.20
	0	13.85	5.87	7.32	11.70	13.37	12.59
	2	45.81	32.57	26.08	40.63	48.99	36.69
	4	44.89	44.23	26.90	73.81	41.31	26.07
0.5	-4	34.41	22.38	33.31	9.75	37.75	63.71
	-2	45.12	16.36	17.15	28.79	35.89	41.36
	0	22.54	8.88	11.22	18.06	20.30	18.97
	2	44.05	27.28	21.54	41.04	39.95	28.90
	4	39.32	38.27	23.53	61.72	36.67	21.79
1	-4	27.56	18.57	27.37	5.31	28.16	51.64
	-2	33.85	13.71	17.00	18.01	27.89	35.35
	0	34.55	12.96	16.48	26.33	29.28	27.20
	2	40.01	21.08	16.62	36.65	30.89	21.32
	4	32.99	31.47	19.31	51.13	30.44	16.17
ort	-4	13.46	9.49	19.49	-5.81	14.18	35.13
	-2	19.24	7.40	10.20	6.64	14.74	21.46
	0	53.67	21.06	26.37	39.53	43.84	40.34
	2	25.56	11.78	9.24	23.87	18.16	10.22
	4	23.60	20.44	10.81	38.02	18.29	6.05

Table 1 presents values of stresses σ_ψ over the cylinder thickness for $a = 2$ within the interval $\psi/32 < \psi < 3\psi/32$ and for $a = 4$ within $\psi/16 < \psi < 3\psi/16$. The Table 1 shows how stresses σ_ψ vary depending on the structure inhomogeneity and cylinder corrugation.

Table 2

		$u_\gamma E_0/q_0$ for $a = 2$				
		ψ	0	$\pi/32$	$2\pi/32$	$3\pi/32$
d	H					
0.1	-4	53.41	51.09	47.12	45.48	45.49
	-2	52.90	50.57	46.61	45.02	45.05
	0	53.63	53.55	53.27	52.89	52.70
	2	62.27	60.63	58.30	58.26	58.91
	4	47.18	53.19	60.95	59.14	55.59
0.25	-4	49.20	47.59	45.25	45.11	45.70
	-2	48.54	46.96	44.67	44.54	45.12
	0	47.64	47.40	47.27	47.78	48.18
	2	51.86	50.58	49.09	49.85	50.82
	4	39.71	44.65	51.39	50.81	48.42
0.5	-4	42.47	41.40	40.16	40.80	41.61
	-2	41.83	40.80	39.60	40.18	40.95
	0	40.87	40.64	40.64	41.44	42.01
	2	43.28	42.28	41.28	42.28	43.28
	4	33.54	37.59	43.32	43.33	41.66
1	-4	33.68	33.01	32.41	33.24	34.00
	-2	33.19	32.55	31.95	32.64	33.30
	0	32.49	32.26	32.22	32.88	33.36
	2	33.74	33.01	32.32	33.14	33.93
	4	26.60	29.68	34.12	34.31	33.15
ort	-4	21.29	20.73	19.79	19.43	19.46
	-2	21.20	20.66	19.60	18.91	18.74
	0	20.20	19.82	18.84	17.79	17.33
	2	19.85	19.15	17.77	16.84	16.59
	4	16.15	17.72	19.47	18.37	17.08

Tables 2 and 3 summarize values of the displacements u_γ over the cylinder thickness for $a = 2$ within the interval $0 < \psi < \pi/8$ (Table 2) and for $a = 4$ within $0 < \psi < \pi/4$ (Table 3) with the isotropic middle layer at $d = 0.1, 0.25, 0.5, 1.0$ and with the orthotropic middle layer. In this case it can be noted, as it follows from Tables 2 and 3, that values of the maximum displacements for the cylinders with the soft middle layer for $d = 0.1$ at $a = 2$ are in the ratio as $0.59 : 1 : 1.8$ while at $a = 4$ as $0.71 : 1 : 2.6$, i.e. they become more pliable in such sequence.

In solving the above problems with construction of the discrete Fourier series for additional functions, we found their values at 80 points taking into account the first 15 harmonics. In this case, to get a stable result by the numerical method used, we adopted 41 orthogonalization points.

Table 3

		$u_\gamma E_0/q_0$ for $a = 4$				
		ψ	0	$\pi/16$	$2\pi/16$	$3\pi/16$
d	H					
0.1	-4	205.73	183.28	143.74	93.68	69.14
	-2	206.31	183.35	142.72	91.49	66.55
	0	206.51	189.30	150.56	100.97	78.04
	2	215.84	200.74	156.89	107.53	85.67
	4	214.24	198.61	155.11	106.40	84.98

0.25	-4	141.60	129.43	110.32	85.71	73.53
	-2	142.04	129.49	109.28	83.45	70.82
	0	141.51	131.24	111.38	86.27	74.28
	2	144.46	134.85	112.81	88.56	77.00
	4	142.92	133.05	111.53	88.08	76.96
0.5	-4	108.28	100.58	89.18	73.46	65.39
	-2	108.83	100.78	88.27	71.33	62.80
	0	108.53	101.33	88.57	71.81	63.48
	2	109.29	102.33	88.65	72.58	64.51
	4	107.91	100.84	87.81	72.59	64.94
1	-4	81.73	76.60	68.72	56.88	50.62
	-2	82.50	77.01	68.03	55.04	48.33
	0	82.47	77.14	67.68	54.57	47.87
	2	82.25	77.03	67.31	54.71	48.21
	4	81.13	75.93	66.97	55.23	49.13
ort	-4	57.47	53.05	44.10	31.15	24.52
	-2	58.56	53.77	43.73	29.81	22.78
	0	58.61	53.45	42.19	27.45	20.13
	2	56.18	51.23	40.11	26.15	19.18
	4	55.39	50.84	40.60	27.48	20.87

Thus, variation in cylinder characteristics makes it possible to choose rational parameters of similar elements of structures.

Conclusions. In conclusion we can note the following. The approach proposed provides an effective tool for constructing solutions of the three-dimensional boundary-value problem concerning equilibrium of hollow noncircular inhomogeneous cylinders of intricate cross-section. For this case we used the Fourier series method for discretely specified functions and stable numerical method of discrete orthogonalization. This approach allowed us to solve the problems for hollow cylinders of various cross-sectional shapes. Besides, the approach being based on a continuous scheme makes it possible to obtain relatively accurate approximate solution. This problem can not be solved by projective or variational methods. The approach was validated in solving problems for single-layered isotropic cylinders with corrugated circular [11] and elliptical [3] cross-sections. The possibility to employment the proposed approach to the solution of problems of the given class has been illustrated by a number of examples. The solution obtained falls in the category of exact solutions of the theory of elasticity which first of all serve as a basis for construction and evaluation of the reliability of applied mathematical models and design schemes as well as for development and estimation of the accuracy of the approximate methods for calculating elements of structures.

1. Годунов С. К. О численном решении краевых задач для систем линейных обыкновенных дифференциальных уравнений // Успехи мат. наук. – 1961. – **16**, № 3. – С. 171–174.
2. Григоренко Я. М. Изотропные и анизотропные слоистые оболочки вращения переменной жесткости. – Киев: Наук. думка, 1973. – 228 с.
3. Григоренко Я. М., Рожок Л. С. К решению задачи о напряженном состоянии полых цилиндров с гофрированным эллиптическим поперечным сечением // Прикл. механика. – 2004. – **40**, № 2. – С. 67–73.
Grigorenko Ya. M., Rozhok L. S. Solving the stress problem for hollow cylinders with corrugated elliptical cross section // Int. Appl. Mech. – 2004. – **40**, No. 2. – P. 169–175.
4. Григоренко Я. М., Рожок Л. С. Расчет напряженного состояния полых цилиндров с гофрами в поперечном сечении // Прикл. механика. – 2002. – **38**, № 12. – С. 72–81.
Grigorenko Ya. M., Rozhok L. S. Stress analysis of corrugated hollow cylinders // Int. Appl. Mech. – 2002. – **38**, No. 12. – P. 1473–1481.
5. Григоренко Я. М., Тимонин А. М. Об одном подходе к численному решению двумерных задач теории пластин и оболочек с переменными параметрами // Прикл. механика. – 1987. – **23**, № 6. – С. 54–61.

- Grigorenko Ya. M., Timonin A. M. An approach to the numerical solution of two-dimensional problems of plate and shell theory with variable parameters // Soviet Appl. Mech. – 1987. – **23**, No. 6. – P. 557–563.
6. Корн Г., Корн Т. Справочник по математике для научных работников и инженеров. – Москва: Наука, 1968. – 720 с.
Korn G. A., Korn T. M. Mathematical handbook for scientists and engineers. – New York: McGraw-Hill, 1961. – 720 p
7. Лехницкий С. Г. Теория упругости анизотропного тела. – Москва: Наука, 1977. – 416 с.
Lekhnitskii S. G. Theory of elasticity of an anisotropic body. – Moskva: Mir, 1981. – 430 p.
8. Семенюк Н. П., Жукова Н. Б., Остапчук В. В. Устойчивость волнообразных некруговых цилиндрических оболочек из композитов при внешнем давлении // Прикл. механика. – 2007. – **43**, № 12. – С. 91–102.
Semenyuk N. P., Zhukova N. B., Ostapchuk V. V. Stability of corrugated composite noncircular cylindrical shells under external pressure // Int. Appl. Mech. – 2007. – **43**, No. 12. – P. 1380–1389.
9. Фихтенгольц Г. М. Курс дифференциального и интегрального исчисления. – Москва: Наука, 1949. – Т. 3. – 783 с.
10. Bellman R. E., Kalaba R. E. Quasilinearization and nonlinear boundary-value problems. – New York: Elsevier, 1965. – 206 p.
11. Grigorenko Ya. M., Rozhok L. S. Discrete Fourier-series method in problems of bending of variable-thickness rectangular plates // J. Eng. Math. – 2003. – **46**, No. 3-4. – P. 269–280.
12. Grigorenko Ya. M., Rozhok L. S. Equilibrium of elastic hollow inhomogeneous cylinders of corrugated elliptic cross-section // J. Eng. Math. – 2006. – **54**, No. 2. – P. 145–157.
13. Hamming R. W. Numerical methods for scientists and engineers. – New York: McGraw-Hill, 1962. – 400 p.
14. Sokolnikoff I. S., Specht R. D. Mathematical theory of elasticity. – New York–London: McGraw-Hill, 1946. – xi + 373 p.
15. Soldatos K. P. Mechanics of cylindrical shells with non-circular cross-section. A survey // Appl. Mech. Rev. – 1999. – **52**, No. 8. – P. 237–274.
16. Timoshenko S. Theory of elasticity. – New York–London: McGraw-Hill, 1934. – 416 p.
Тимошенко С. П. Теория упругости. – Ленинград–Москва: ОНТИ, 1934. – 451 с.

РІВНОВАГА ПРУЖНИХ ПОРОЖНИСТИХ НЕОДНОРІДНИХ ЦИЛІНДРІВ З ПОПЕРЕЧНИМ ПЕРЕРІЗОМ У ВИГЛЯДІ ОПУКЛИХ НАПІВГОФРІВ

Наведено розв'язок тривимірної крайової задачі теорії пружності про напружений стан порожнистих неоднорідних ортотропних циліндрів з поперечним перерізом у вигляді опуклих напівгофрів із зонами значної кривизни. Граничні умови на торцях циліндра дозволяють відокремити змінні в напрямку довжини. У розв'язувальну систему диференціальних рівнянь вводяться доповняльні функції, які дозволяють відокремити змінні вздовж напрямної за рахунок використання дискретних рядів Фур'є. Отримана крайова задача для системи звичайних диференціальних рівнянь розв'язується стійким чисельним методом дискретної ортогоналізації по товщині циліндра. Наводяться результати розв'язання задачі у вигляді графіків і таблиць.

РАВНОВЕСИЕ УПРУГИХ ПОЛЫХ НЕОДНОРОДНЫХ ЦИЛИНДРОВ С ПОПЕРЕЧНЫМ СЕЧЕНИЕМ В ВИДЕ ВЫПУКЛЫХ ПОЛУГОФРОВ

Представлено решение трехмерной краевой задачи теории упругости о напряженном состоянии полых неоднородных ортотропных цилиндров с поперечным сечением в виде выпуклых полугофров с зонами большой кривизны. Граничные условия на торцах цилиндра позволяют разделить переменные по длине. В разрешающую систему дифференциальных уравнений вводятся дополнительные функции, которые позволяют разделить переменные по направляющей за счет использования дискретных рядов Фурье. Полученная краевая задача для системы обыкновенных дифференциальных уравнений решается устойчивым численным методом дискретной ортогонализации по толщине цилиндра. Приводятся результаты решения задачи в виде графиков и таблиц.

S. P. Timoshenko Inst. of Mechanics
of NAS of Ukraine, Kiev

Received
05.12.13